Electronic Supporting Information

Precise design of dual active-site catalysts for synergistic catalytic therapy of tumor

Guodong Cheng[1,4,5], Fuying Chen[1,4], Shulian Li[2], Yu Hu[3], Zhichao Dai[1,4], Zunfu Hu[1,4], Zibao Gan[1,4], Yunqiang Sun[1,4*], Xiuwen Zheng[4,5*]

[1] College of Chemistry and Chemical Engineering, Linyi University, Linyi 276000, P. R. China

[2] Linyi Cancer Hospital, Linyi, 272067, P. R. China.

[3] Zhucheng City People's Hospital, Zhucheng, 262200, P. R. China.

[4] Key Laboratory of Functional Nanomaterials and Technology in Universities of Shandong, Linyi University, Linyi 276000, P. R. China

[5] Qilu Normal University, Jinan, 250013, P. R. China.

*Corresponding authors

E-mail: Yunqiang Sun, sunyunqiang@lyu.edu.cn; Xiuwen Zheng, zhengxiuwen@lyu.edu.cn

Table of Contents

1. Experimental

1.1 Materials

1,1-bis (diphenylphosphine) ferrocene dichloride platinum dichloromethane was purchased from Sinocompound catalysts Co, Ltd. Fe (III) acetylacetonate (Fe(acac)$_3$, 98%), Pt(II) acety-lacetonate (Pt(acac)$_2$, 98%),and hydrogen peroxide (H$_2$O$_2$, 30%) were purchased from Beijing HWRK Chem. Dimethyl formamide (DMF), glacial acetic acid (HAc), and methanol (CH$_3$OH, 99.9%) were obtained from Shanghai Chemical Reagents, China.3,3′,5,5′-tetramethylbenzidine dihydrochloride hydrate (TMB) were purchased from Sigma-Aldrich Co. Ltd. HA was purchased from Shangdong Freda Biopharm Co. Ltd. Cell Counting Kit-8 (CCK-8) were purchased from Beyotime Biotechnology. Cy5-NHS ester was purchased from Dalian Meilun Biotechnology Co., Ltd. The Calcein-AM/Propidium Iodide (PI) Staining Kit was purchased from Invitrogen (USA). Deionized water was used in the experiments. All the chemicals used in the present study were of analytical grade, and they were used without further purification.

1.2 Characterization

TEM (HRTEM) images were determined on a JEOL-2100 transmission electron microscope. The structure and morphology of the prepared samples were examined using a sub-angstrom resolution high-angle annular dark-field scanning transmission electron microscope (HAADF-STEM) on a Titan cubed G260-300 with an accelerating voltage of 200 kV, equipped with two Cs-correctors (probe and image Cs-correctors). High-angle annular dark-field (HAADF)-scanning transmission electron microscopy (STEM) coupled with EDS elemental mapping was conducted on a JEOL ARM-200F field emission transmission electron microscope. X-ray diffraction (XRD) patterns were obtained from a Smart Lab X-ray diffractometer (RIGAKU) using Cu Kα radiation (λ =

0.15418 nm). The metal content in the catalyst was measured by inductively coupled plasma-mass spectrometry (ICP-MS). Dynamic light scattering (DLS) and Zeta potential were detected by Nano-ZS (Malvern). X-ray photoelectron spectroscopy (XPS) was conducted on a Thermo ScientificTM K-AlphaTM+ spectrometer equipped with a monochromatic Al Kα X-ray source (1486.6 eV) operating at 100 W. Samples were analyzed under vacuum ($P < 10^{-8}$ mbar) with a pass energy of 150 eV (survey scans) or 50 eV (high-resolution scans). All peaks would be calibrated with C1s peak binding energy at 284.8 eV for adventitious carbon. The X-ray absorptio finestructure (XAFS) was conducted using the 8 C nanoprobe XAFS beamline (BL8C) of Pohang light source (PLS-II) in the 3.0 GeV storage ring, with a ring current of 250 mA. The X-ray beam was monochromated by a Si (111) double crystal where the beam intensity was reduced by 30% to eliminate the higher-order harmonics. The X-ray beam was then delivered to a secondary source aperture where the beam size was adjusted to be 0.5 mm (v) × 1 mm (h). The XAFS spectra were collected in both transmission and fluorescence modes. The obtained spectra were processed using a Demeter software. For wavelet transform (WT) analysis, the χ(k) exported from Athena was imported into the Hama Fortran code The UV-vis spectra were carried out on a NANO DROP 2000 spectrophotometer, respectively.

1.3 Synthesis of Fe-SAC/NC, Pt-SAC/NC and NC.

Fe-SAC/NC and Pt-SAC/NC were prepared by replacing 1,1-bis(diphenylphosphino)ferrocene dichloride platinum dichloromethane complexes with the same molar amounts of iron acetylacetonate and platinum acetylacetonate, respectively, according to the same procedure. Direct pyrolysis of COF at the same temperature to obtain NC.

1.3 Synthesis of Fe-SAC/NC@HA, Pt-SAC/NC@HA and NC@HA.

Fe-SAC/NC@HA, Pt-SAC/NC@HA and NC@HA preparation method was similar to that of FePt-DAC/NC@HA.

2. Experimental Details

2.1 Catalysts poisoning experiment.

It has been reported that anions like SCN^- would poison the metal active center, and such poison effect has been applied as an important method to judge the existence of the metal-N active site. Fe-SAC/NC, Pt-SAC/NC and FePt-DAC/NC (100 µg mL^{-1}) and 0.2 M KSCN were added into a tube. The poisoning time of the catalyst was set as 30 minutes to guarantee the poisoning effect. Then 20 mM H_2O_2 was added and incubated for 60 minutes. $Ti(SO_4)_2$ terminational assay was used to calculate the degradation rate of H_2O_2. As calculated using equation:

$$H_2O_2(\%) = \frac{At}{A0} \times 100\%$$

Where A0 and At represent experimental group and blank group，respectively.

2.2 TMB chromogenic assays.

The effect of pH on the catalytic activity of FePt-DIA/NC was measured by adding 100 µg mL^{-1} FePt-DIA/NC, 20 mM H_2O_2 and 1 mM TMB to PBS buffers of pH 5.8, pH 7.4 and pH 8.2, respectively. The reaction solution was allowed to react for 5 minutes at room temperature and the final absorbance at 652 nm was measured using a UV detection instrument. The catalytic properties of the different materials were tested in buffer solutions of pH 5.8 according to the same procedure.

The contents of FePt-DAC/NC and Fe-SAC/NC were converted according to the metal ion content. The concentration of SACs (C_{SACs}) was calculated using equation:

$$C_{SACs} = C_{FePt-DAC/NC} \times Metal\ element\ contents\ \%$$

where "metal element contents %" was measured using ICP-MS (Table. S1).

2.3 Detection of ROS by ESR.

For the detection of •OH, FePt-DAC/NC, Fe-SAC/NC, or Pt-SAC/NC (final concentration: 100 µg mL^{-1}) was mixed with an aqueous reaction system containing 10 mM H_2O_2 and BMPO (1 mM) by vortexing for 30 seconds, followed by the recording of ESR spectra.

2.4 Photothermal Conversion Effect of FePt-DAC/NC.

The photothermal conversion effect was fully investigated at different condition: the solution FePt-DAC/NC ([FePt-DAC/NC] = 100 µg mL^{-1}) was irradiated by 808-nm laser at different power of 0.8, 1.0, 1.1 and 1.2 W cm^{-2}. Different concentration of FePt-DAC/NC ([FePt-DAC/NC] = 50, 100, 200 and 300 µg mL^{-1}) were irradiated by 808-nm laser at power of 1.2 W cm^{-2}.

2.5 Calculation of the Photothermal Conversion Efficiency.

The photothermal conversion efficiency of FePt-DAC/NC the was determined according to the previous method[1]. The η value was calculated as follows:

$$\eta = \frac{hS(T_{max} - T_{surr}) - Q_{dis}}{I(1 - 10)^{-A_{808}}} \times 100\%$$

Where h is the heat transfer coefficient, S is the surface area of the container, T_{max} is the equilibrium temperature, T_{surr} is the ambient temperature, I is the incident laser power, A_{808} is the

absorbance of FePt-DAC/NC solution at 808-nm. The value of hS can be obtained using the following equation

$$hS = \frac{m_w C_w}{\tau_s}$$

Where m_w is the mass of water, C_w is the heat capacity of water, τ_s is the time constant of the sample system.

According to Fig. 4h, τ_s was determined and calculated to be 145.3s. Thus, substituting according values of each parameters into：

$$\eta = \frac{0.40 \times \dfrac{4.2}{145.3}(60.3 - 23.8) - 0.00081}{1.2 \times (1 - 10^{-1.0386})} \times 100\% = 38.6\%$$

2.6 Cell Culture.

4T1 and MCF-7 cells were incubated in DMEM medium involving 10% FBS, 20 mM HEPES, 2 mM L-glutamine, 100 U mL^{-1} streptomycin and 100 U/mL penicillin at 37℃ under 0.1% O_2 and 5% CO_2.

2.7 In Vitro Cell Cytotoxicity.

4T1 cells, MCF-7 cells and LO2 cells (both 1×10^4 cells) were seeded into 96-well plate cultured for 10 hours, respectively. Subsequently, 20 μL different concentrations (12.5, 25, 50, 100, 200 μg mL^{-1}) of FePt-DAC/NC@HA was added into wells on the plate. Then 10 μL CCK-8 (5 mg mL^{-1}) was added to ach well and incubated for 30-60 minutes in incubator (37 ℃, 5% CO_2) and the absorbance of the cells at 450 nm was detected by micro-plate reader. The cell viability of Pt-SAC/NC@HA and Fe-SAC/NC@HA were also estimated with similarly treatment. About the laser irradiation group, after the 4T1 or MCF-7 cells cultured by different treatments at different

concentrations (FePt-DAC/NC@HA=12.5, 25, 50, 100, 200 µg mL^{-1}) for 6 houurs, the laser irradiation was carried out at 808-nm (1.2 W cm^{-2}) for 5 minutes, and continue to culture for 4 hours.

The cell viability was calculated according to the equation:

$$Cell\ viability\ (\%) = \frac{A_0 - A_t}{A_0} \times 100\%$$

Where A_0 and A_t represent experimental group and blank group, respectively.

2.8 Determination of ROS generation in vitro.

The fluorescent probe of 2'7'-dichlorofluorescin diacetate (DCFH-DA) reagent were used to detect ROS. After incubation with PBS, Pt-SAC/NC@HA (25 µg mL^{-1}), Fe-SAC/NC@HA (25 µg mL^{-1}), and FePt-DAC/NC@HA (25 µg mL^{-1}) for 6 h, the 4T1 cells were washed twice with PBS. Then, 1 mL of DMEM containing DCFH-DA and Hochest 33342 was added, and the cells were cultured for another 30 min. After being washed thrice with PBS, 4T1 cells stained with DCFH-DA (green) and Hoechst 33342 (blue) were fluoresced under an inverted microscope.

2.9 Live/dead staining assay.

The 4T1 tumor cells were cultured in 12-well plates and exposed to various treatments, including PBS, Pt-SAC/NC@HA, Fe-SAC/NC@HA, FePt-DAC/NC@HA, FePt-DAC/NC@HA, and FePt-DAC/NC@HA + 808-nm Laser. Laser exposure (1.2 W cm^{-2}) was implemented for 5 minutes. After being washed thrice with PBS, 4T1 cells were incubated with calcein-AM/PI. Finally, 4T1 cells were washed thrice with PBS and fluoresced under an inverted microscope.

2.10 In vivo fluorescence imaging.

FePt-DAC/NC@HA- Cy5 was intravenously injected into Balb/c mice with tumors. The mice were then placed in an imaging device and fluorescence images were obtained at various time intervals after injection. The mice were euthanized 12 hours after injection, and fluorescence images and fluorescence intensity of major organs were obtained.

2.11 Hemolysis Assay.

The blood sample (0.2 mL) was donated by a single mouse. Red blood cells (RBCs) were collected by centrifugation at 3000 rpm for 5 minutes, washed with PBS for 3 times, and resuspended using PBS (10 mL) to prepare the 2% RBC suspension. Then, different concentrations of FePt-DAC/NC@HA suspensions (FePt-DAC/NC@HA: 20, 40, 80, 100 and 200 μg mL^{-1}; PBS as the solvent) were separately mixed with 2% RBC suspensions in equal volumes in centrifuge tubes. After being incubated at 37 °C for 2 hours, the supernatants were obtained through centrifugation at 3000 rpm for 5 minutes. RBCs in PBS and water were used as a negative control and a positive control, respectively.

2.12 In Vivo Synergistic Anticancer Study.

All the animal procedures were performed in compliance with the guidelines of the Institutional Animal Care and Use Committee of Department of Laboratory Animal Science, Linyi University. To assess the treatment effect, 4T1 tumor-bearing Balb/c mice with tumor volumes of approximately 100 mm^3 were selectively divided into 7 groups (n = 5) and treated with PBS, PBS + 808-nm Laser (1.2 W cm^{-2}), NC@HA, NC@HA + 808-nm Laser (1.2 W cm^{-2}), Fe-SAC/NC@HA, FePt-DAC/NC@HA and FePt-DAC/NC@HA + 808-nm Laser (1.2 W cm^{-2}) treatments. NC@HA, Fe-SAC/NC@HA and FePt-DAC/NC@HA in PBS (100 μL) dose of 20 mg

kg^{-1}. PBS solution containing nanomaterial was injected intravenously into the mice through the tail vein every 2 days. The tumor volume and weight of the mice were recorded before the next injection. After treatment, mice were euthanized, and major organs and tumors were obtained for terminal deoxynucleotidyl transferase dUTP nick end labeling (TUNEL), hematoxylin and eosin (H&E) staining.

Tumor volumes were counted using equation：

$$Tumor\ volumes = \frac{L \times W^2}{2}$$

where L (mm) and W (mm) refer to the length and width of the tumor, respectively.

2.13 Study on the distribution of Fe/Pt in organisms.

Three mice with similar weights were euthanised by intravenous injection of FePt-DAC/NC@HA nanocatalyst for 36 h. The heart, liver, spleen, lungs, kidneys and tumors were collected and placed in a vacuum oven for drying to remove excess water. The viscera were powdered separately with a mortar and pestle, dispersed into aqua regia and dissolved for 24 hours. It was diluted the same number of times with three times of water, filtered and the content of Fe and Pt in each organ and tumors was determined by ICP-MS.

3. Supplementary Figures.
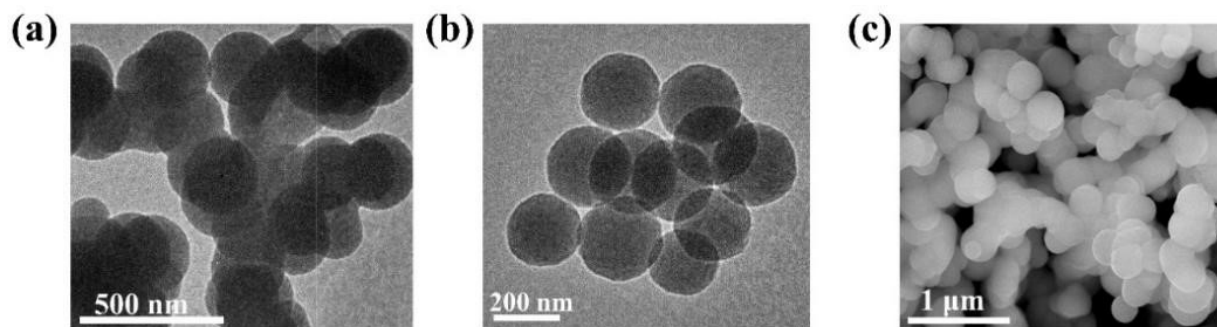
Fig. S1 (a) and (b)TEM image of COF; (c) SEM image of COF.
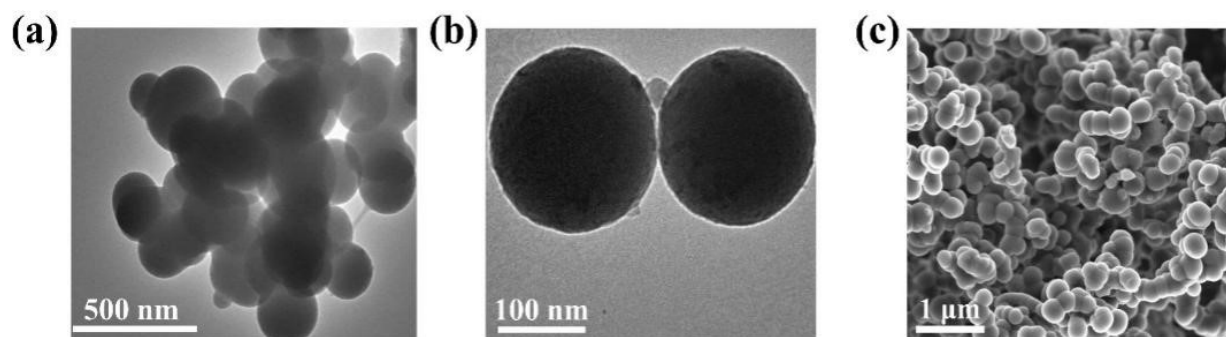
Fig. S2 (a) and (b) TEM image of Fe-SAC/NC. (C) SEM image of Fe-SAC/NC.
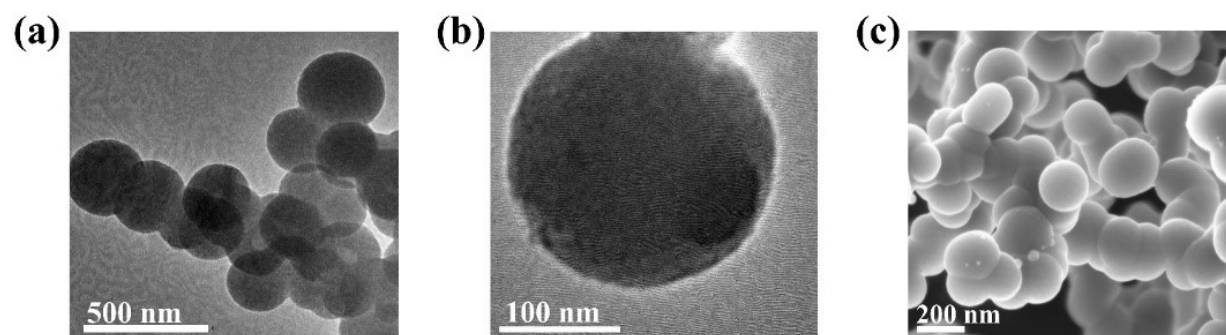
Fig. S3 (a) and (b) TEM image of Pt-SAC/NC. (C) SEM image of Pt-SAC/NC.
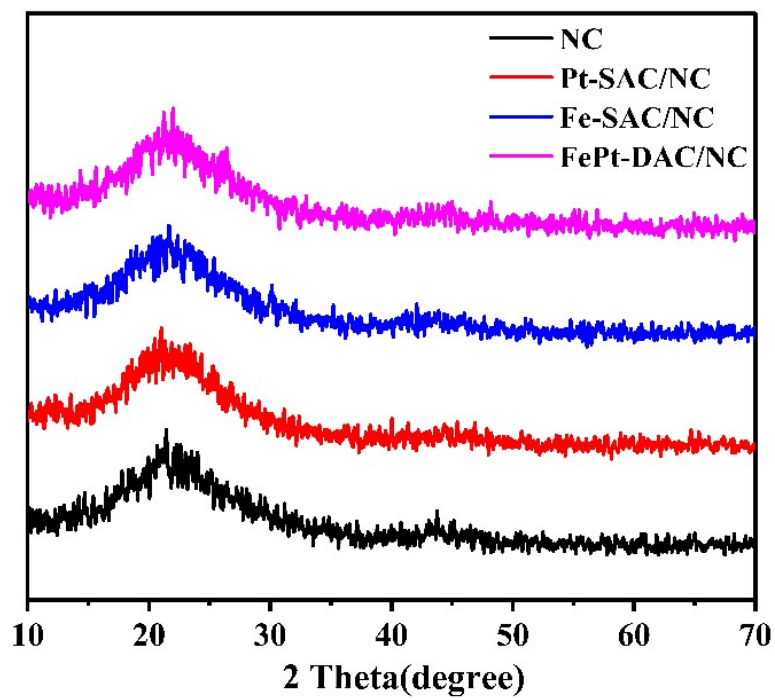
Fig.S4 XRD patterns of NC, Pt-SAC/NC, Fe-SAC/NC, and FePt-DAC/NC
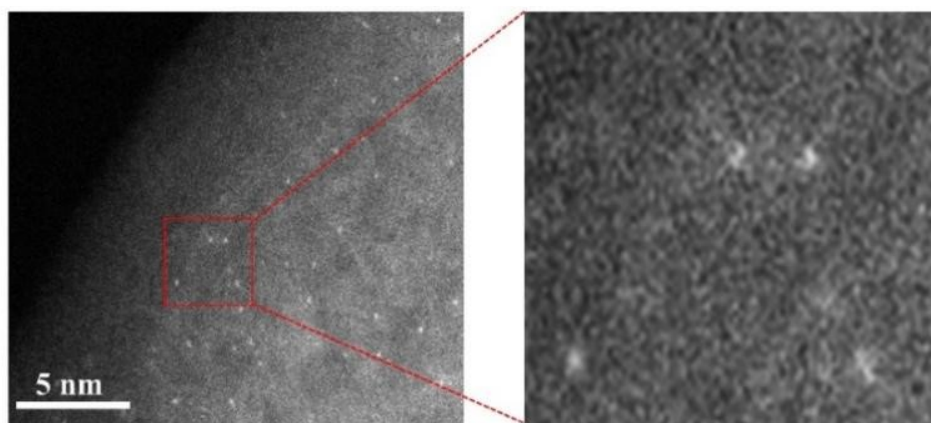
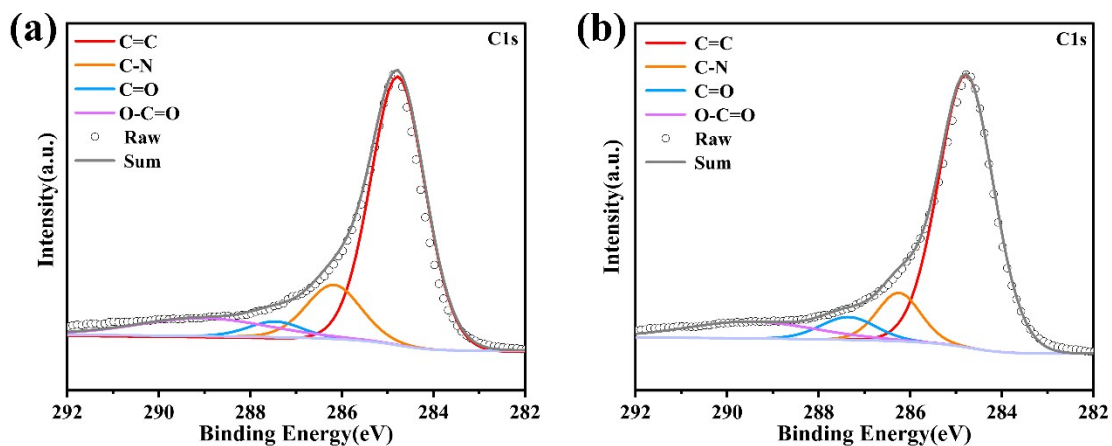**Fig. S5** Atomic-resolution HAADF-STEM images of Fe-SAC/NC.
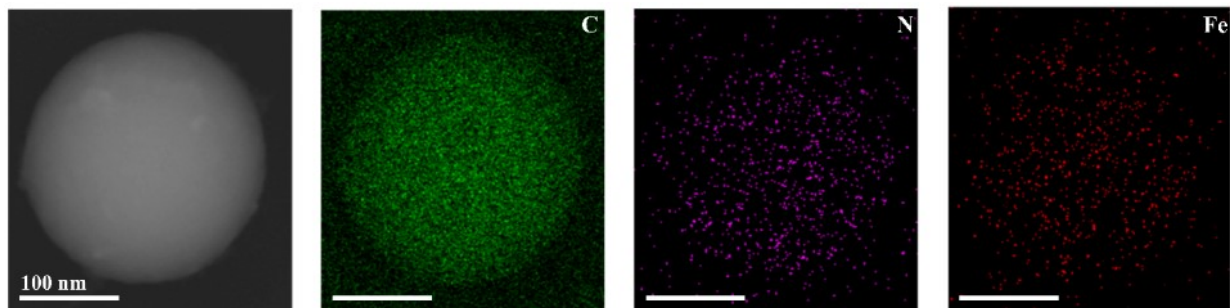
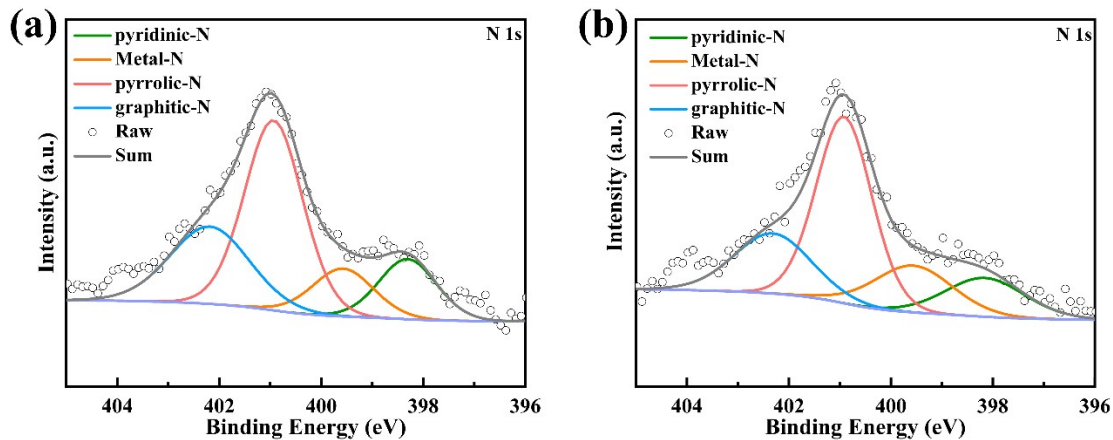**Fig. S6** TEM-EDS mapping images for Fe-SAC/NC (scale bar: 100 nm).
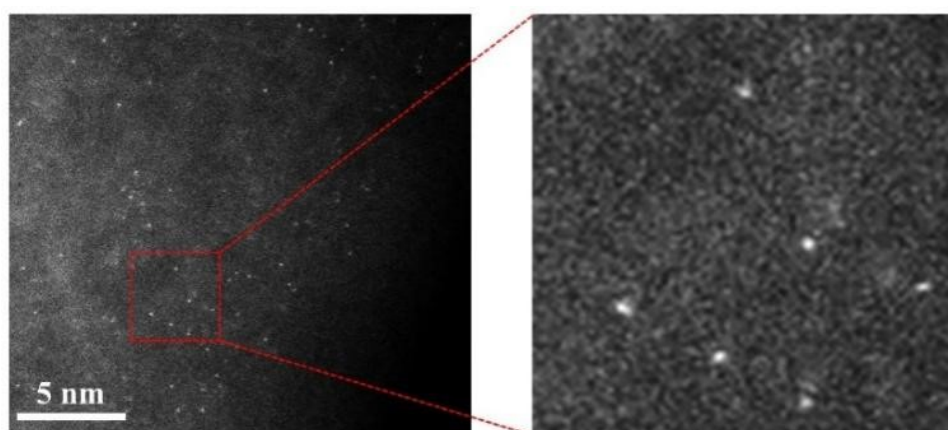
Fig. S7 Atomic-resolution HAADF-STEM images of Pt-SAC/NC
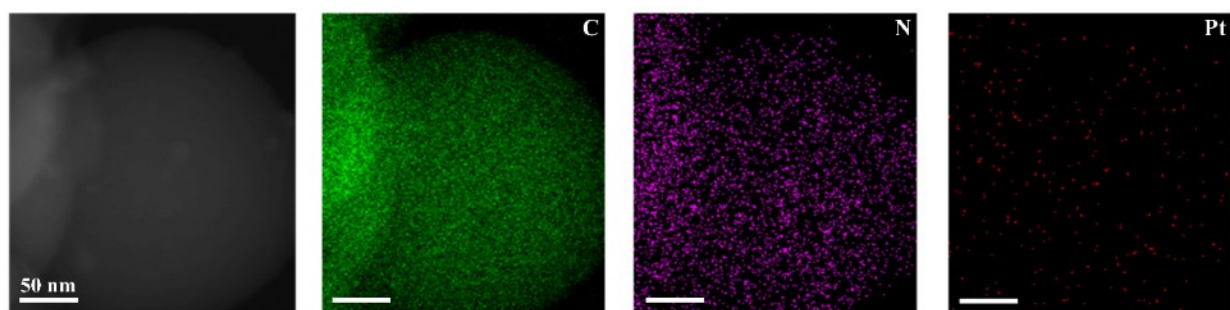
Fig. S8 TEM-EDS mapping images for Pt-SAC/NC (scale bar: 50 nm).

Fig. S9 (a) XPS spectra for C 1s of Fe-SAC/NC. (b) XPS spectra for C 1s of Pt-SAC/NC.

Fig. S10 (a) XPS spectra for the N 1s region of Fe-SAC/NC. (b) XPS spectra for the N 1s region of Pt-SAC/NC.
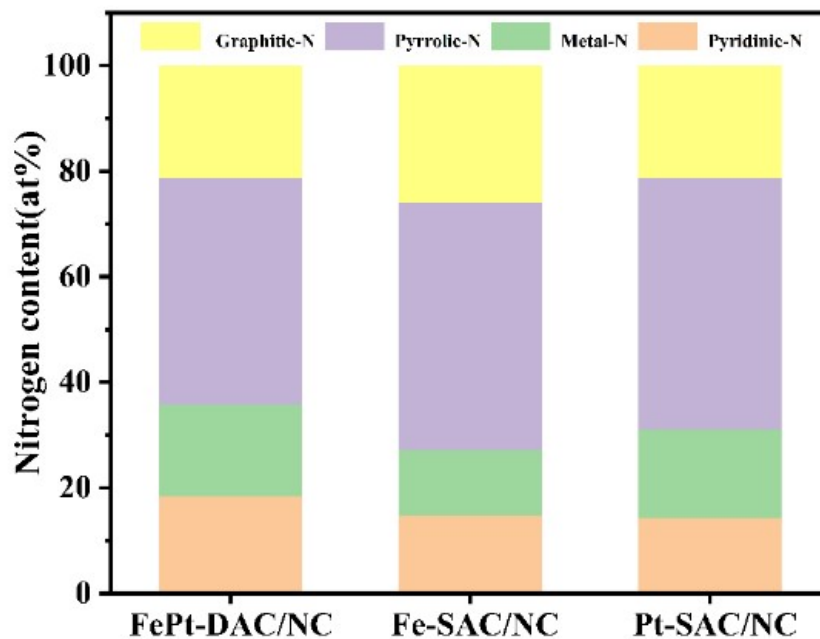
Fig. S11 Various nitrogen content profile of FePt-DAC/NC, Fe-SAC/NC and Pt-SAC/NC.
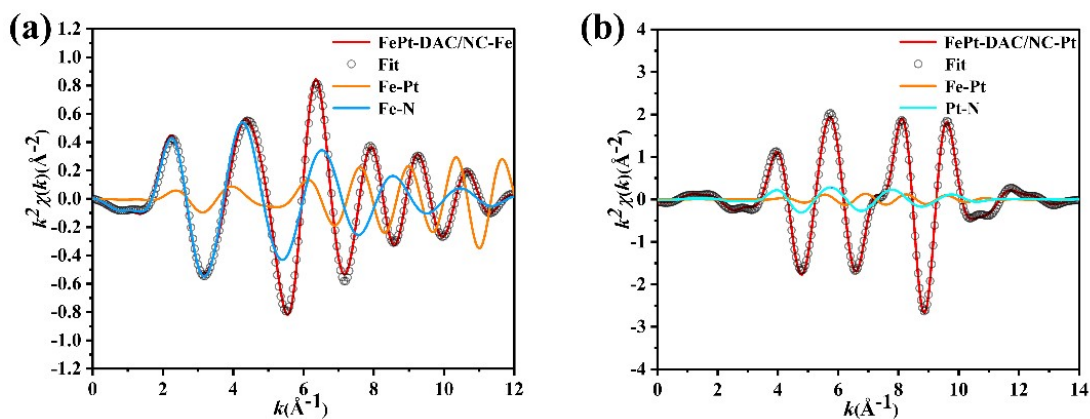
Fig. S12 (a) k space fitting curves of Fe with the Fe-N$_3$ configuration. (b) k-space fitting curves of Pt with the Pt-N$_3$ configuration.
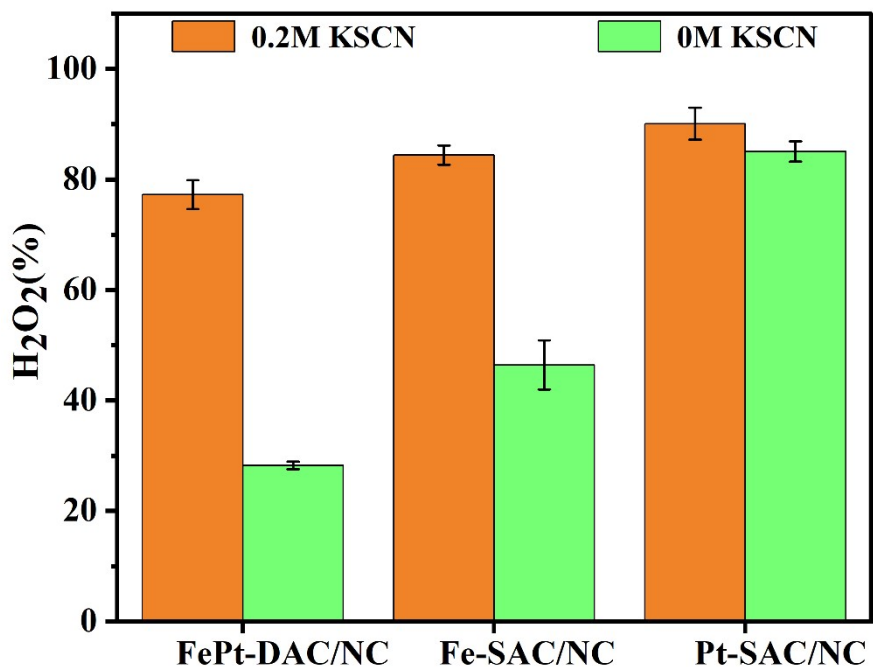
Fig. S13 The catalytic activity of FePt-DAC/NC, Fe- SAC/NC and Pt-SAC/NC with/without KSCN in the presence of H_2O_2 using $Ti(SO_4)_2$ assy.
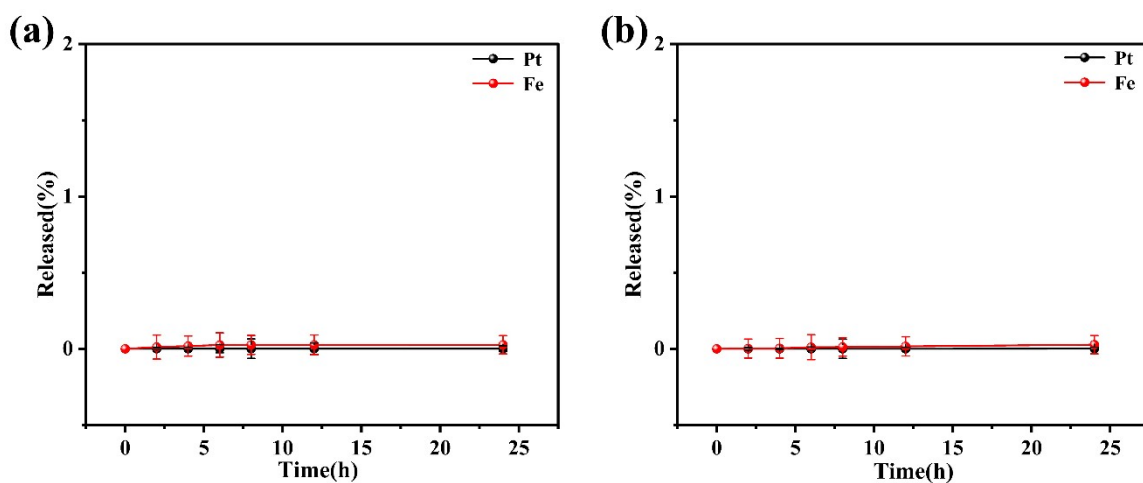
Fig. S14 (a) The Fe ions and Pt ions release behavior of FePt-DAC/NC (1mg/mL) at pH 5.8 measured by ICP-MS analysis; (b) The Fe ions and Pt ions release behavior of FePt-DAC/NC (1mg/mL) at pH 7.4 measured by ICP-MS analysis.
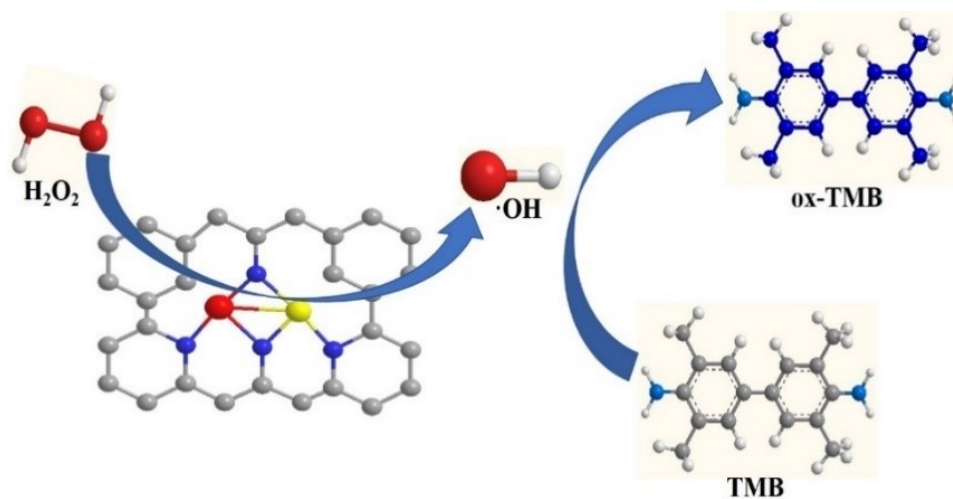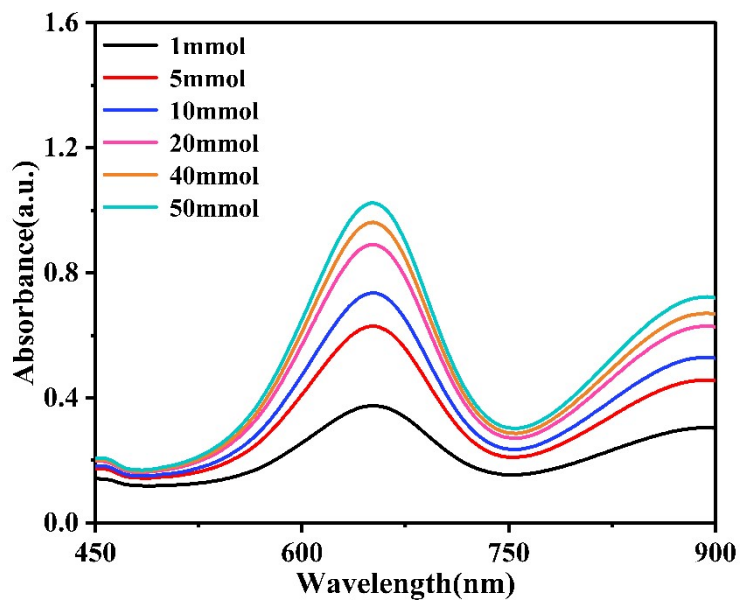
**Fig. S15** Schematic illustration of the catalytic activity of FePt-DAC/NC.
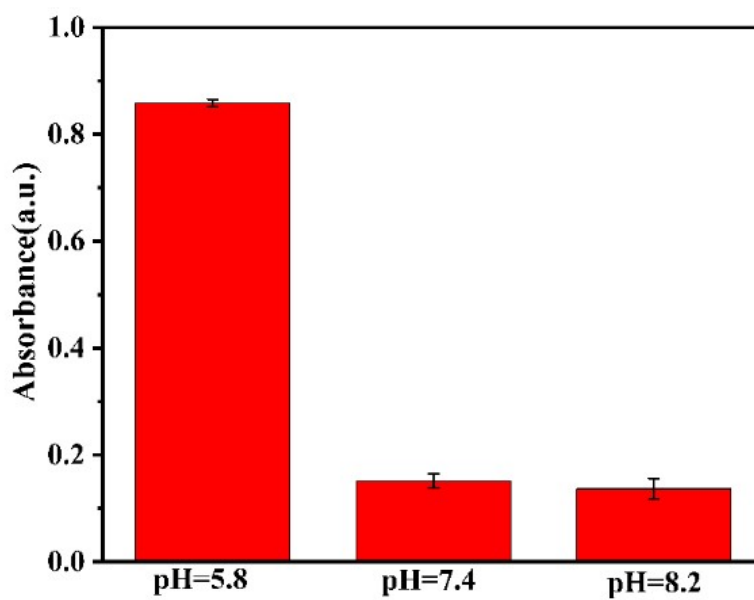
Fig. S16 3,3'5,5'-tetramethylbenzidine (TMB) assay for measuring catalytic activity of the mentioned catalysts at different pH values in the presence of H_2O_2.
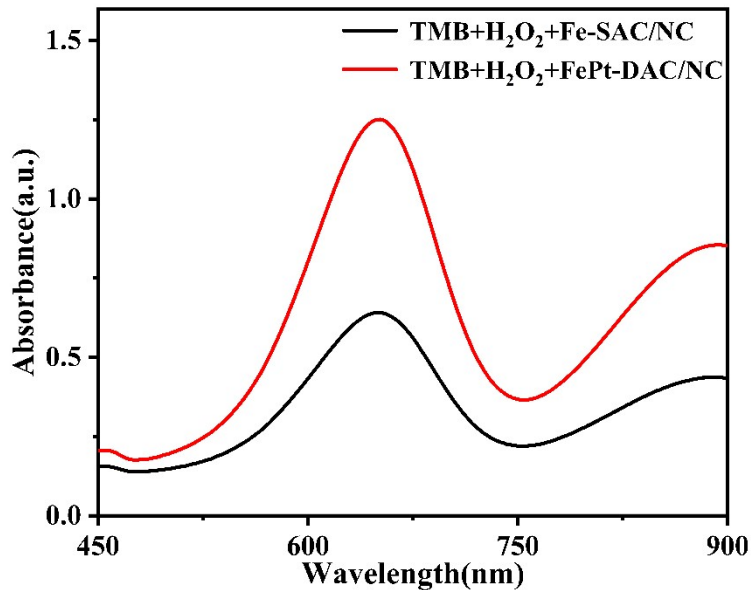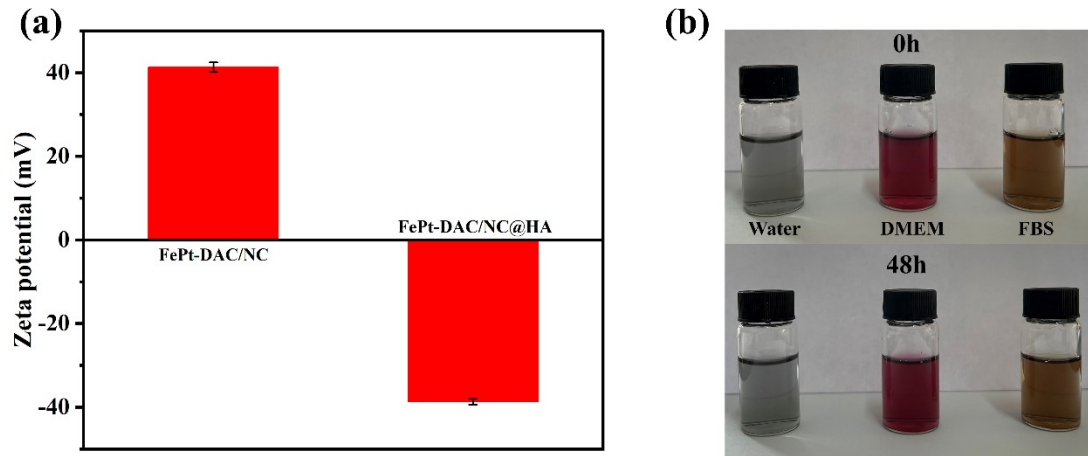
Fig. S17 UV-vis spectra of FePt-DAC/NC oxidised TMB at pH 5.8 after conversion based on the content of iron ions in Fe-SAC/NC.
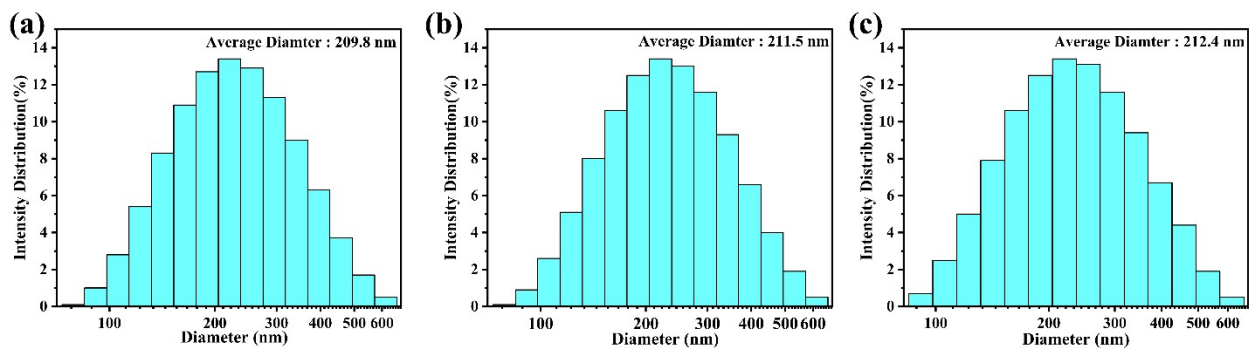

Fig. S18 Validation experiments of hydroxyl radical production at different hydrogen peroxide concentrations at pH 5.8.
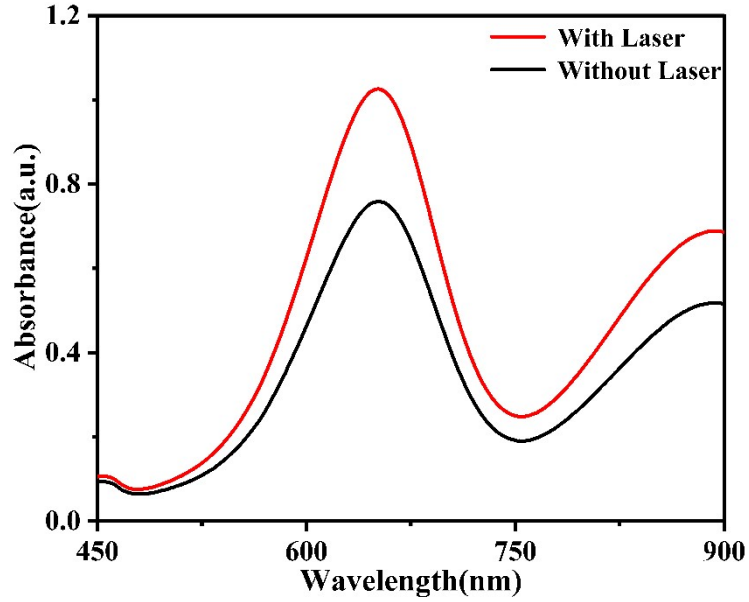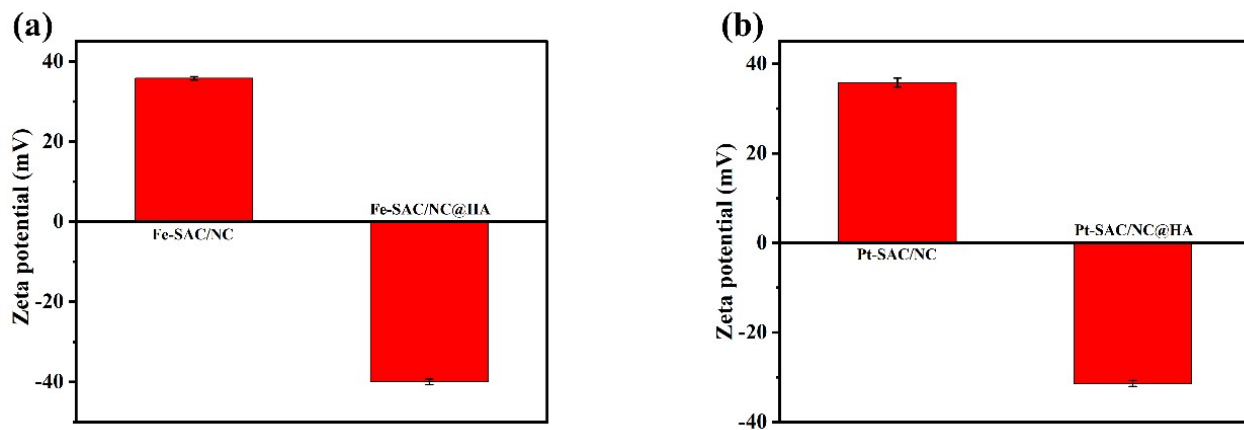
Fig. S19 UV-vis spectra of TMB + H_2O_2 + FePt-DAC/NC with or without 808 nm laser irradiation.
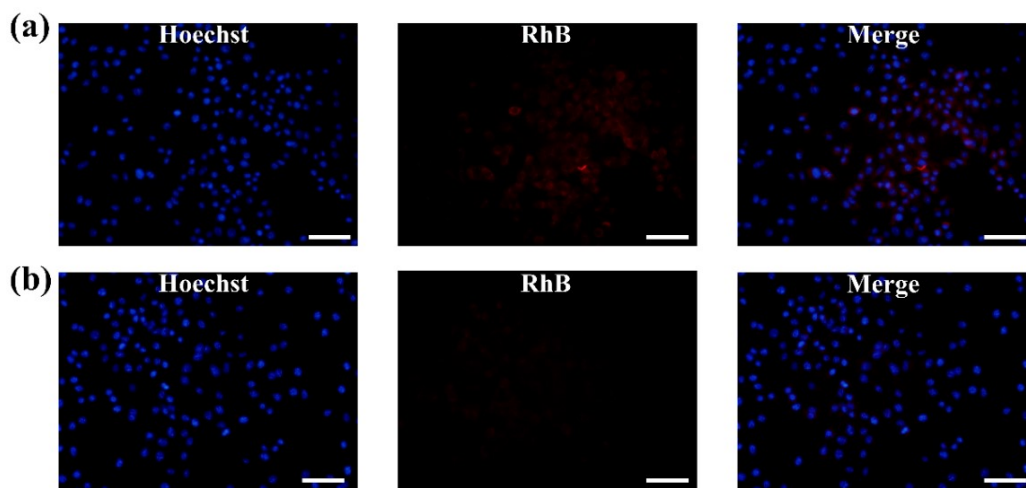

Fig. S20 (a) Zeta potential of FePt-DAC/NC and FePt-DAC/NC@HA. (b) The stability image dispersed in Water, DMEM and FBS of FePt-DAC/NC@HA.

Fig. S21 (a) Dynamic light scattering (DLS) of as prepared FePt-DAC/NC@HA. (b) The DLS of FePt-DAC/NC@HA stand for 24 hours and (c) 48 hours.
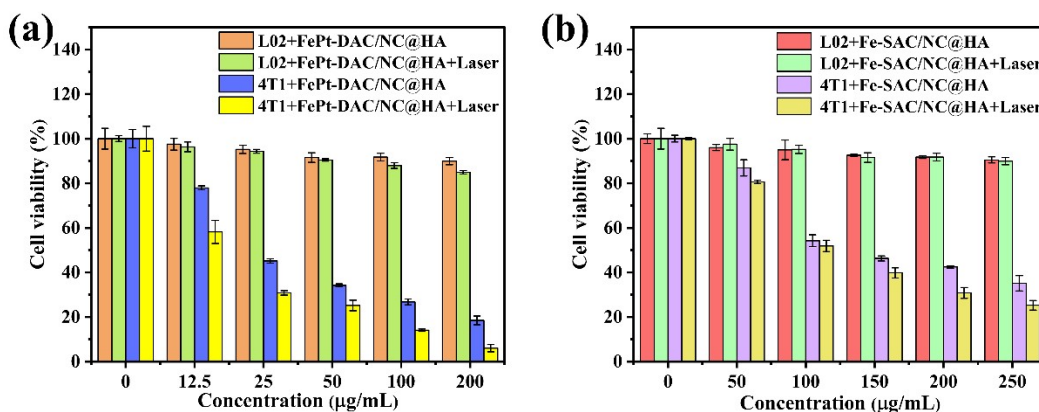

Fig. S22 Zeta potential of (a) Fe-SAC/NC and Fe-SAC/NC@HA, and (c) Pt-SAC/NC and Pt-SAC/NC@HA.

Fig. S23 (a) Fluorescence microscopy images showing the uptake of FePt-DAC/NC@HA-RhB and (b) FePt-DAC/NC-RhB by cells after coculture with 4T1 cells for 4 hours (scale bar: 100 μm).
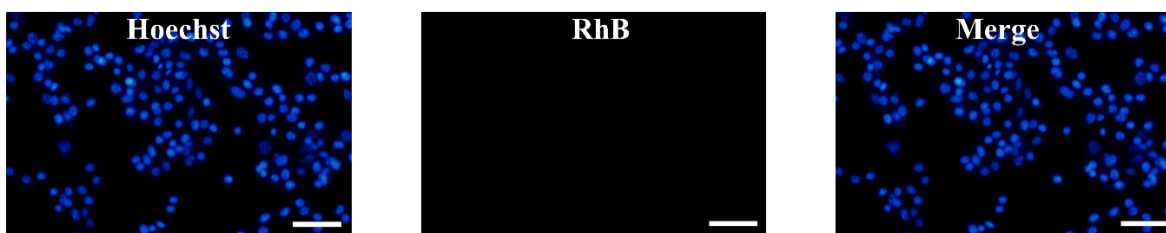

Fig. S24 Fluorescence images of L02 cells incubated with FePt-DAC/NC@HA-RhB for 4 h (scale bar: 100 μm).


Fig. S25 (a) Cell viabilities of L02 cells and 4T1 cells with or without laser and different concentrations of FePt-DAC/NC@HA. (b) Cell viabilities of L02 cells and 4T1 cells with or without laser and different concentrations of Fe-SAC/NC@HA.
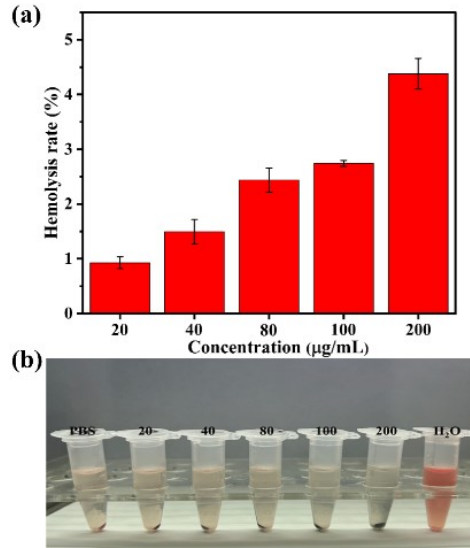
Fig. S26 (a) Corresponding hemolysis rates of the RBC samples; (b) Photograph of RBC suspensions after treatment with various concentrations of FePt-DAC/NC@HA. The RBC suspensions treated with PBS and H_2O were set as negative control and positive control, respectively.
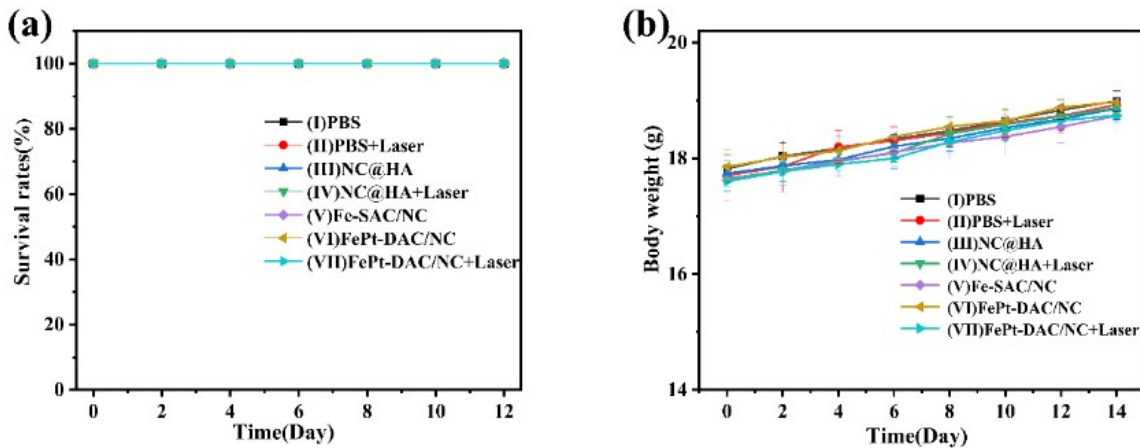
Fig. S27 (a) Survival rates and (b) body weight curves of BALB/c mice during the treatment (n = 5).
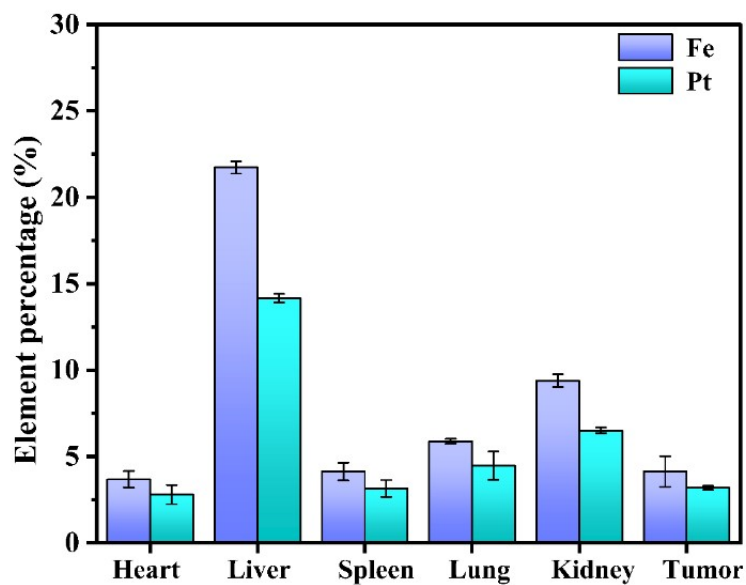
Fig. S28 The biodistribution of Fe and Pt in tumors and major organs measured by ICP-MS after intravenous injection with FePt-DAC/NC@HA for 36 h.
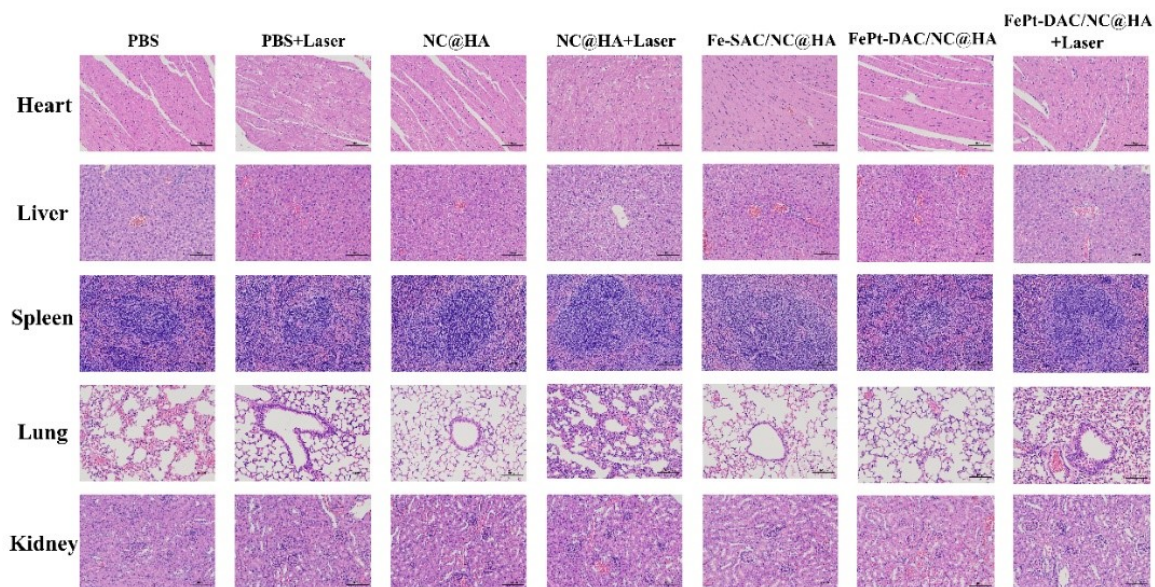
Fig. S29 H&E staining for nuclear dissociation in major organs. (Scale bars: 100 μm).

4. Supplementary Table.

Table S1. ICP-MS results for Pt and Fe contents in the as-prepared Fe-SAC/NC, Pt-SAC/NC and FePt-DAC/NC.

Sample	FePt-DAC/NC	Fe-SAC/NC	Pt-SAC/NC
Fe countent (wt%)	0.43	0.63	
Pt countent (wt%)	0.17		0.24

Table S2. EXAFS fitting parameters at the M K/L_3-edge for various samples.

Sample	Shell	CN[a]	R(Å)[b]	σ^2(Å^2)[c]	ΔE_0(eV)[d]	R factor
			Fe K-edge			
Fe	Fe-N	2.7±0.4	1.992±0.019	0.0133±0.0033	0.6±2.5	0.0141
	Fe-Pt	0.9±0.2	2.598±0.029	0.0042±0.0020	-6.6±3.4	
			Pt L_3-edge			
Pt	Pt-N	2.9±0.3	1.967±0.024	0.0057±0.0054	8.0±5.7	0.0033
	Pt-Fe	1.2±0.5	2.602±0.023	0.0093±0.0043		

[a]CN, coordination number; [b]R, the distance to the neighboring atom; [c]σ^2, the Mean Square Relative Displacement (MSRD); [d]ΔE_0, inner potential correction; R factor indicates the goodness of the fit. $S0^2$ was fixed to 0.716 and 0.828, according to the experimental EXAFS fit of Fe foil and Pt foil by fixing CN as the known crystallographic value[2]. * This value was fixed during EXAFS fitting, based on the known structure of Fe and Pt[3]. Fitting range: $2.0 \leq k$ (/Å) ≤ 12.0 and $1.0 \leq R$ (Å) ≤ 3.5 (Fe); $3.0 \leq k$ (/Å) ≤ 13.2 and $1.0 \leq R$ (Å) ≤ 3.0 (Pt). A reasonable range of EXAFS fitting parameters: $0.700 < S_0^2 < 1.000$; $CN > 0$; $\sigma^2 > 0$ Å^2; $|\Delta E_0| < 10$ eV; R factor < 0.02.

4. Supplementary References

1 Y. Xing, J. Xiu, M. Zhou, T.; Xu, M. Zhang, H. Li, X. Li, X.; Du, T. Ma and X. Zhang, *ACS Nano*, 2023, **17**, 6789-6799.
2 B. Ravel and M. Newville, *J Synchrotron Rad*, 2010, **12**, 537-541.
3 H. Funke, M. Chukalina, and A. Rossberg, *Phys Scripta*, 2005, **T115**, 232-234.